Inactivating *NF1* Mutations Are Enriched in Advanced Breast Cancer and Contribute to Endocrine Therapy Resistance

Alex Pearson[1], Paula Proszek[2], Javier Pascual[1], Charlotte Fribbens[1], Monee K. Shamsher[1], Belinda Kingston[1], Ben O'Leary[1], Maria T. Herrera-Abreu[1], Rosalind J. Cutts[1], Isaac Garcia-Murillas[1], Hannah Bye[2], Brian A. Walker[2], David Gonzalez De Castro[2], Lina Yuan[2], Sabri Jamal[2], Mike Hubank[2], Elena Lopez-Knowles[1,3], Eugene F. Schuster[1,3], Mitch Dowsett[1,3], Peter Osin[4], Ashutosh Nerurkar[4], Marina Parton[4], Alicia F.C. Okines[4], Stephen R.D. Johnston[4], Alistair Ring[4], and Nicholas C. Turner[1,4]

ABSTRACT

Purpose: Advanced breast cancer (ABC) has not been subjected to the same degree of molecular scrutiny as early primary cancer. Breast cancer evolves with time and under the selective pressure of treatment, with the potential to acquire mutations with resistance to treatment and disease progression. To identify potentially targetable mutations in advanced breast cancer, we performed prospective molecular characterization of a cohort of patients with ABC.

Experimental Design: Biopsies from patients with advanced breast cancer were sequenced with a 41 genes targeted panel in the ABC Biopsy (ABC-Bio) study. Blood samples were collected at disease progression for circulating tumor DNA (ctDNA) analysis, along with matched primary tumor to assess for acquisition in ABC in a subset of patients.

Results: We sequenced 210 ABC samples, demonstrating enrichment compared with primary disease for potentially targetable mutations in *HER2* (in 6.19% of samples), *AKT1* (7.14%), and *NF1* (8.10%). Of these enriched mutations, we show that *NF1* mutations were frequently acquired in ABC, not present in the original primary disease. In ER-positive cancer cell line models, loss of *NF1* resulted in endocrine therapy resistance, through both ER-dependent and -independent mechanisms. NF1 loss promoted ER-independent cyclin D1 expression, which could be therapeutically targeted with CDK4/6 inhibitors *in vitro*. Patients with *NF1* mutations detected in baseline circulating tumor DNA had a good outcome on the CDK4/6 inhibitor palbociclib and fulvestrant.

Conclusions: Our research identifies multiple therapeutic opportunities for advanced breast cancer and identifies the previously underappreciated acquisition of *NF1* mutations.

Introduction

As breast cancer evolves from primary to metastatic breast cancer, and through the selective pressure of treatment, the genetic drivers may change (1, 2). The genomics of primary breast cancer has been well established through multiple large studies including The Cancer Genome Atlas (TCGA; ref. 3) and Molecular Taxonomy of Breast Cancer International Consortium (4), and yet the acquired genetic events of advanced breast cancer have been investigated less thoroughly (5). Mutations in the estrogen receptor (ER) are acquired in advanced ER-positive breast cancer, especially during treatment with aromatase inhibitors (6, 7). Mutation in the estrogen receptor influences sensitivity to subsequent endocrine therapies, suggesting that acquired genetic events may be critical to predicting outcome on subsequent therapy.

Breast cancer is characterized by a large number of relatively rare genetic events that may both predict for adverse outcome and be potentially targetable with novel therapies. Yet few studies have examined how these genetic events may change in metastatic breast cancer, whether such genetic events may be enriched through inherent poor prognosis, and therefore relative enrichment, or through acquisition by tumor evolution. Here in a clinical sequencing program, we identify acquired mutations in the *NF1* tumor suppression gene in advanced breast cancer, demonstrating that such mutations are enriched in the metastatic setting.

NF1 is a tumor suppressor gene that encodes for neurofibromin protein, which acts as a repressor of RAS-GTP activation, with loss of NF1 resulting in RAS activation and downstream to the MAPK pathway activation (8). *NF1* germline mutations are associated with neurofibromatosis type 1 (NF1), a dominant autosomal disorder clinically characterized by pigmentary changes in the skin and typically the apparition of multiple peripheral nerve sheath tumors (neurofibromas) and other benign nervous system tumors like optic gliomas. Germline *NF1* mutation increases the risk of breast cancer especially in women under 50 years old that could lead to an increased risk of cancer-related death (9–11). Somatic mutations in *NF1* are rare in primary cancer, but are associated with poor prognosis and an increased risk of recurrence (12). Loss of *NF1* expression results in tamoxifen resistance in preclinical models (13). Here we elucidate the functional consequences of *NF1* loss in

[1]Breast Cancer Now Toby Robins Research Centre, The Institute of Cancer Research, London, United Kingdom. [2]The Centre for Molecular Pathology, The Royal Marsden Hospital, Sutton, Surrey, United Kingdom. [3]Ralph Lauren Centre for Breast Cancer Research, Royal Marsden Hospital, London, United Kingdom. [4]Breast Unit, The Royal Marsden Hospital, London, United Kingdom.

Note: Supplementary data for this article are available at Clinical Cancer Research Online (http://clincancerres.aacrjournals.org/).

Corresponding Author: Nicholas C. Turner, Breast Cancer Now Toby Robins Research Centre, Institute of Cancer Research and The Royal Marsden Hospital, Fulham Road, London SW3 6JJ, United Kingdom. Phone: 207-811-8914; Fax: 207-352-5441; E-mail: nick.turner@icr.ac.uk

Clin Cancer Res 2020;26:608–22

doi: 10.1158/1078-0432.CCR-18-4044

Translational Relevance

We show that the molecular profile of advanced breast cancer is enriched for multiple potentially targetable genetic events, which are associated with poor prognosis and resistance to adjuvant therapy, with increased frequency of *HER2, AKT1*, and *NF1* mutations. Among these, truncating mutations in *NF1* can be selected in advanced breast cancer, not present in original matched primaries, and are associated with poor prognosis and endocrine resistance that may be overcome through inhibition of CDK4/6.

ER-positive breast cancer and identify therapeutic approaches to treat *NF1* mutations.

Materials and Methods

Study design and patients

Patients with advanced breast cancer were recruited into a clinical sequencing study, the Advanced Breast Cancer Biopsy (ABC-Bio) trial (CCR3991, REC ID: 14/LO/0292), a prospective tissue collection study at The Royal Marsden Hospital (London, United Kingdom). The study protocol was approved by the NHS Health Research Authority, Research Ethics Committee London-Chelsea. Written informed consent was obtained from each patient in accordance with regulatory requirements, good clinical practice, and the Declaration of Helsinki. Patients consented to either a biopsy of metastatic disease or access to an archival biopsy of recurrent disease. Blood was collected in EDTA blood tubes at disease progression for circulating tumor DNA (ctDNA) analysis. IHC analysis and assessment of tumor samples was performed by the Histopathology Department, Royal Marsden Hospital (London, United Kingdom). ER and PR scoring were assessed following the Allred/Quick Score, which gives a scoring range of 0–8. Scores 3–8 were considered positive. In cases with ER^-, only a strong score in PR (defined as >5) allocated the sample as hormone receptor positive (HR^+). IHC analyses of HER2 were reported as a score ranging from 0 to 3. Scores 0 and 1+ were considered negative, 3+ positive, and borderline 2+ results were retested with *in situ* hybridization methods to confirm HER2 positivity. Cases included using external analysis had been performed under standard local practice and according to general recommendations.

Additional paired samples before and after resistance to aromatase inhibitors (AI) were collected in a retrospective tissue collection study, the AI pairs study. These paired tumor biopsy samples were obtained from patients pre- and postprogression (either locally advanced or metastatic disease) while receiving treatment with an AI (14, 15). A total of 48 paired samples were subjected to molecular characterization by next-generation sequencing and gene expression analysis (15).

Baseline plasma samples from the PALOMA-3 trial were analyzed. PALOMA-3 was a multicenter, randomized phase III trial assessing palbociclib and fulvestrant in premenopausal and postmenopausal women ($n = 331$) with advanced, HR–positive breast cancer who had progressed during prior endocrine therapy, as reported previously (16). Patients were assigned 2:1 to palbociclib (125 mg orally for 3 weeks followed by 1 week off) and fulvestrant (500 mg intramuscularly every 14 days for the first three injections, then 500 mg every 28 days), or matching placebo plus fulvestrant. Written informed consent was obtained from all participants.

Next-generation sequencing

Formalin-fixed paraffin-embedded (FFPE) tissue blocks were reviewed for tumor content by a pathologist and tumor-rich areas marked. Tumor sections were macrodissected to enrich for tumor content.

DNA was extracted from 10-μm sections of FFPE tumor samples using QIAamp DNA FFPE tissue kit (56404, Qiagen) and quantified using the Qubit dsDNA High Sensitivity Assay Kit with the Qubit 3.0 fluorometer (Invitrogen). Samples were sequenced using a targeted capture panel (The Breast NGS v1.0 panel) consisting of 41 breast cancer driver genes (Supplementary Table S1) selected on the basis of either being frequently mutated in breast cancer or rare but potentially targetable (3, 17, 18). NGS libraries were prepared from 50–400 ng DNA using the KAPA HyperPlus Kit (Kapa Biosystems) and SeqCap EZ adapters (Roche, NimbleGen), following the manufacturer's protocol, including dual solid-phase reverse immobilization size selection of the libraries (250–450 bp). To optimize enrichment and reduce off-target capture, pooled, multiplexed, amplified precapture libraries (up to 13 samples per hybridization) were hybridized overnight using 1 μg of total DNA to a custom design of DNA baits complementary to the genomic regions of interest (NimbleGen SeqCap EZ library, Roche). Hybridized DNA was PCR amplified and products purified using AMPure XP beads (Beckman Coulter) and quantified using the KAPA Quantification Q-PCR Kit (KAPA Biosystems).

Sequencing was performed on a MiSeq (Illumina) with 75-bp paired-end reads and v3 chemistry, or NextSeq (Illumina) with 75 bp paired-end reads and v2 chemistry, according to the manufacturer's instructions. For samples where germline matched control was available, pools from tumor and control DNA libraries were multiplexed separately for hybridization and combined prior sequencing at a ratio of 4:1, increasing the relative number of reads derived from tumor DNA.

Miseq runs were analyzed using MiSeq Reporter Software (v2.5.1; Illumina), to generate nucleotide sequences and base quality scores in Fastq format. Resulting sequences were aligned against the human reference genome build GRCh37/Hg19 to generate binary alignment (BAM) and variant call files (VCF). Secondary analysis was carried out using Molecular Diagnostics Information Management System to generate quality control, variant annotation, data visualization, and a clinical report. Reads were deduplicated using Picard (http://broadinstitute.github.io/picard/), and metrics generated for each panel region. Oncotator (v1.5.3.0) (https://software.broadinstitute.org/cancer/cga/oncotator) was used to annotate point mutations and indels using a minimum variant allele frequency (VAF) of 5% and a minimum number of 10 variant reads as a cutoff (19). Manta (https://github.com/Illumina/manta) was used for the detection of structural variants (20). Variants were annotated for gene names, functional consequence (e.g., Missense), PolyPhen-2 predictions, and cancer-specific annotations from the variant databases including COSMIC (https://cancer.sanger.ac.uk/cosmic), Tumorscape (21), and published MutSig results (22). Copy number variation (CNV) was assessed by measuring the coverage ratio between each tumor probe target and the average coverage of all probe targets in the normal (when a normal sample was available). If a normal sample was not available the ratio between each tumor probe target and the average of all probe targets in the tumor was used instead. Ratios below 0.5-fold were defined as a potential deletion, whereas a ratio above 2.4 was flagged as a potential amplification if 80% of the target regions had exceeded the thresholds. Borderline genes with less than but almost 80% of the targets showing amplification/deletion were not automatically flagged but assessed individually. All potential mutations, structural

variants, and CNVs were visualized using Integrative Genomics Viewer (IGV; refs. 23, 24) and two individuals were required to review the mutation report independently. VCF files from unpaired samples were annotated using Illumina VariantStudio v3.0, and checked manually on IGV.

NextSeq runs were analyzed using an in-house pipeline. For demultiplexing, bcl2fastq (v2.19) was used to isolate reads for each sample. The reads were aligned to the reference genome build GRCh37/Hg19 using Burrows–Wheeler Aligner (BWA-MEM), followed by the marking of PCR duplicates and calculation of various QC metrics using Picard. Copy number was estimated as described above for the analysis of Miseq runs. Manta (v.0.29.6) was used for the detection of structural variants. Genom Analysis ToolKit (GATK) was used for realigning around indels to improve indel calling and base quality score recalibration for adjusting systematic errors made by the sequencer when estimating quality scores of each base call (25). Finally, GATK was also used for variant calling using HaplotypeCaller for tumor only analysis (limit of detection ~10%) and MuTect2 for tumor paired analysis. VCF files from unpaired samples were annotated using Illumina VariantStudio v3.0, and checked manually on IGV.

The Breast NGS v1.0 panel could detect single-nucleotide variants at >5% allele frequency with >99% sensitivity (95% CI) and >98% specificity (95% CI). Small indels could be detected with sensitivity >95% and specificity >81% at >5% variant allele frequency. High-level gene amplifications (>8 copies) could be detected in samples with >30% neoplastic nuclei. For each patient, germline DNA was sequenced to allow subtraction of single-nucleotide polymorphisms, thus only somatic variants were reported.

The sequencing strategies used in the molecular characterization of ctDNA in the PALOMA3 study are described in detail by O'Leary and colleagues (26).

Mutation detection using digital droplet PCR

ctDNA was extracted from plasma using either the QIAamp circulating nucleic acid kit (Qiagen) or the QIASymphony SP Instrument using QIAsymphony DSP Circulating DNA Kit (Qiagen) according to manufacturer's guidelines. Concentrations of extracted ctDNA were estimated using either a TaqMan Copy Number Reference Assay (4403326, Life Technologies) for *RPPH1* (27–29) or the Qubit hsDNA quantification kit and Qubit instrument (Life Technologies). Mutations in *PIK3CA* (p.E542K, *c.1624G>A*; p.E545K, *c.1633G>A*; p.H1047R, *c.3140 A>G*; p.H1047L, *c.3140A>T*; ref. 26) and *ESR1* (p.E380Q, *c.1138G>C*; p.L536R, *c.1607T>G*; p.Y537C, *c.1610A>G*; p/D538G, *c.1613A>G*. p.S463P, *c.1387T>C*; p.Y537N, *c.1609T>A*; p.Y537S, *c.1610A>C*) were interrogated by digital PCR (dPCR) using custom assays as described previously (6, 26, 27, 30). *AKT1* hotspot mutation (p.E17K, *c.49G>A*) was interrogated using a commercial dPCR kit (dHsaCP2000031 and WT: dHsaCP2000032, Bio-Rad) as per the manufacturer's instructions and dPCR was conducted as described previously (14).

RNA extraction and NanoString gene expression on tumors

RNA was extracted from tumor samples using RNeasy Mini Kit (74104, Qiagen) and quantified using the Qubit RNA High Sensitivity Assay Kit with the Qubit 3.0 fluorometer (Life Technologies). RNA from tumors with *NF1* mutations was run on a NanoString nCounter with a custom codeset comprised of 70 genes (Supplementary Table S2; ref. 15), according to the manufacturer's guidelines. Expression data from *NF1*-mutant samples was combined and normalized with an existing expression dataset (AI pairs study cohort, $n = 30$), generated using the same codeset (15). The AI pairs cohort contained 3 *NF1*-mutant tumors, expression data from which were added to the ABC-bio *NF1*–mutant dataset.

Cell lines

MCF7 and T47D cell lines were obtained from ATCC and cultured in phenol-free RPMI media (32404-014, Life Technologies) supplemented with 10% dextran/charcoal-stripped FBS (12676029, Life Technologies), 1 nmol/L estradiol (Sigma), glutamine (25030149, Life Technologies), penicillin and streptomycin (15140-122, Life Technologies). Cell lines were banked in multiple aliquots on receipt to reduce risk of phenotypic drift and identity confirmed by short tandem repeat profiling with the PowerPlex 1.2 System (Promega).

Antibodies, RNAi, and drugs

Antibodies used were phosphorylated (p) AKT S473 (4058), pAKT T308 (2965), AKT (4691), CCND1 (2978), CCNE1 (4129), CCNE2 (4132), pCDK2 T160 (2561), CDK2 (2546), pERa S118 (2511), pERa S167 (64508), ERa (13258), pERK1/2-Thr202/Tyr204 (4370), ERK1, 2 (9102), NF1 (14623), pRB S780 (3590), pRB S807 (8516), Rb (9313), PGR (8757), p-mTOR S2481 (2974), mTOR (2983), phospho-ribosomal protein S6 (5364), ribosomal protein S6 (2217; all Cell Signaling Technology). Fulvestrant (S1191), tamoxifen (S1238), and palbociclib (S1116) were obtained from Selleck Chemicals. siRNAs were from Dharmacon: siGENOME nontargeting siRNA Pool#2 (D-001210-02), siGENOME NF1 set of 4 (MQ-003916-03). NF1 shRNA constructs, shLuc-72243, shNF1-39714, and shNF1-39717 (31, 32) were a kind gift from Dr. Steven Whittaker (Institute of Cancer Research, London, United Kingdom). The vectors were packaged into lentivirus in 293-T cells and MCF7 cells were infected with shLuc-72243 MCF7-LucB2.2, shNF1-39714 (MCF7-shNF1_14B2.2), and shNF1-39717 (MCF7-shNF1_17B2.2). At 96 hours after infection, 2 μg/mL puromycin was added and a polyclonal stable pool was established under continuous selection.

Gene expression using dPCR

cDNA was prepared using the SuperScript III First Strand Kit (Life Technologies; 18080-051) according to the manufacturer's guidelines, using 50 to 200 ng total RNA primed with random hexamers. dPCR gene expression reactions were typically set up with 1 to 5 ng RNA equivalent of cDNA. Taqman gene expression assays for *NF1* (Hs01035108_m1), *NCOR1* (Hs01094541_m1), and *NCOR2* (Hs00196955_m1) were run a duplex reaction and normalized using *GUSB* reference assay (Hs99999908_m1) were obtained from Life Technologies Ltd. dPCR was conducted as described previously (14).

Human estrogen receptor RT^2 profiler PCR array

RNA was extracted from cells using RNeasy Mini Kit (74104, Qiagen), and genomic DNA eliminated and cDNA prepared with 500 ng template RNA using RT^2 First strand Kit (330401, Qiagen), according to manufacturer's guidelines. cDNA samples were prepared for qPCR using RT^2 SYBR Green qPCR Mastermix (330523, Qiagen) and run on the Human Estrogen Receptor RT^2 Profiler PCR Array (330231, PAHS-005ZA-24, Qiagen) comprising 84 target genes and 5 housekeeping genes (Supplementary Table S3). For each sample, gene expression data were adjusted using the geometric mean of the housekeeping genes, the ΔC_t calculated and data presented as the $\log_2$ fold change.

Western blotting

Cells were lysed in NP40 lysis buffer (1% v/v NP40, 10 mmol/L Tris–HCl pH8, 150 mmol/L NaCl, 1 mmol/L EDTA, 1 mmol/L DTT) supplemented with protease/phosphatase inhibitor cocktail (5872, Cell Signaling Technology). Western blots were carried out with

precast TA or Bis-Tris gels (Life Technologies). Cells were reverse transfected with siRNA 72 hours prior to lysis.

Colony formation assays

Colony formation assays were conducted in 6-well plates, seeded with 1,000–2,500 cells prior to exposure to the indicated experimental conditions. Plates were fixed with tricyclic acid (10%), stained with sulforhodamine B (SRB), and colonies counted using a GelCOUNT instrument (Oxford Technologies).

Bromodeoxyuridine incorporation assays

Cells were seeded into 96-well plates and S-phase fraction assayed after 24 hours exposure to compounds, with the addition of 10 μmol/L bromodeoxyuridine (BrdU) for 2 hours prior to fixing. BrdU incorporation was assessed with Cell Proliferation Chemiluminescent ELISA-BrdUrd Assay (Roche 11 669 915 001) according to the manufacturer's instructions and adjusted for viable cells in parallel wells assessed with CellTiter-Glo (33, 34).

Statistics, databases, and analysis tools

Mutation and expression data from TCGA (Provisional, 1,105 samples) was extracted from cBioPortal (http://www.cbioportal.org/; refs. 35, 36). Only ER-positive samples were extracted and the remaining samples were divided into NF1-truncated and nontruncating with samples with missense *NF1* mutations removed from the analysis. Data were normalized and differential expression was investigated between *NF1*-mutated and nonmutated samples using the voom function from the LIMMA R package. Further pathways analysis on the differentially expressed genes was carried out using Ingenuity pathway analysis (Qiagen, https://www.qiagenbioinformatics.com/products/ingenuity-pathway-analysis/). Graphical presentation of mutations in context with protein domains was performed using ProteinPaint (https://pecan.stjude.cloud/pp). Other statistical analysis was performed as indicated using GraphPad Prism v7.05 and custom scripts in R version 3.4.3. Correction for multiple comparisons was performed using either Sidak test for multiple comparisons or the method of Benjamini–Hochberg for false discovery as indicated. Survival analysis was performed using log rank test for *P* values and Mantel-Haenszel method for hazard ratios.

Results

Genetic profile of advanced breast cancer

A total of 246 patients with metastatic breast cancer gave consent and were recruited into a clinical sequencing study (ABC-Bio study, **Fig. 1A**), with sequencing data obtained for 210 patients. The clinical demographics of the 210 patients are shown in **Table 1**. Sequencing revealed mutations in 33 genes, including *TP53* (44.8%, 98 mutations in 94 patients), *PIK3CA* (37.1%, 93 mutations in 78 patients), *ESR1* (10.0%, 22 mutations in 21 patients), *NF1* (8.1%, 17 mutations in 17 patients), *HER2* (6.2%, 13 mutations in 13 patients), and *AKT1* (7.1%, 16 mutations in 15 patients; **Fig. 1B**). Comparison with the mutation incidence in primary cancers in the TCGA dataset, revealed higher mutations rates in ABC in *TP53* ($q = 0.0011$), *ESR1* ($q = 5.26 \times 10^{-11}$), *NF1* ($q = 0.0078$), *AKT1* ($q = 4.76 \times 10^{-9}$), *HER2* ($q = 0.0207$), *PTEN* ($q = 0.0195$), and *SF3B1* ($q = 0.041$; all Fisher exact test with FDR correction using Benjamini–Hochberg method; **Fig. 1B**).

Of the mutations found at higher frequency in ABC, *NF1* was characterized by frequent inactivating, truncating, or nonsense mutations (**Fig. 1C**). *AKT1* and *HER2* were dominated by known hotspot-activating mutations, while in *PTEN* frameshift, nonsense, and deletions accounted for the majority of identified mutations (**Fig. 1B**; Supplementary Fig. S1A). *ESR1* mutations were found at a high prevalence only in HR-positive/HER2-negative tumors (20/22 mutations $HR^+/HER2^-$, $P = 0.0278$, Fisher exact test; Supplementary Fig. S1A). $HR^+/HER2^-$ tumors had significantly lower incidence of *TP53* mutations (40/143, 27.97%) than both $HER2^+$ tumors (16/19, 84.21%, $P < 0.0001$, Fisher exact test) and triple-negative breast cancer (TNBC; 37/45, 82.22%, $P < 0.0001$; Fisher exact test), with subtype determined in metastatic sample. $HR^+/HER2^-$ tumors had a similar rate of *PIK3CA* mutations (57/143, 39.86%) to $HER2^+$ tumors (7/19, 36.84%), and nonsignificantly higher rate than TNBC (12/45, 26.67%, $P = 0.1555$, Fisher exact test), in part, as compared with metastatic TNBC, which in turn had a higher rate of *PIK3CA* mutations than primary TNBC in TCGA. Incidence of *NF1* mutations was similar in $HR^+/HER2^-$, $HER2^+$ tumors and TNBC (Supplementary Fig. S1A). Comparison of mutation frequency between ABC-Bio and TCGA by tumor subtype showed comparable mutation frequencies with significant increase identified in *ESR1* and *AKT1* in $HR^+/HER2^-$ tumors after adjusting for multiple comparisons. The rate of *NF1* mutations increased from 2.5% in TCGA to 7.0% in ABC-Bio ($P = 0.021$, $q = 0.127$; Supplementary Fig. S1B). Similarly, ABC-Bio sequencing was highly comparable with the MSKCC dataset (37), with increased frequency of mutations noted in *ESR1, AKT1*, and *BRCA1* compared with primary breast cancers (Supplementary Fig. S1C). *HER2* amplification status had very high agreement with clinical *HER2* amplification status determined by IHC or FISH (sensitivity = 1, specificity = 0.9746, $P < 0.0001$: Supplementary Fig. S1D).

We next looked at factors that influenced the genomic profile. *ESR1* mutations were only rarely identified in patients with newly relapsed disease, and were frequent in patients with more heavily pretreated cancer (Supplementary Table S4). Similarly, *ESR1* mutations were rare in *TP53*-mutant advanced $HR^+/HER2^-$ breast cancer (1/40) and common in *TP53* wild-type $HR^+/HER2^-$ breast cancer (18/142, 12.6%, $P = 0.0455$ Fisher exact test, **Fig. 2A**). This suggested that *ESR1* mutations are acquired through prior endocrine therapy in the metastatic setting, principally in *TP53* wild-type cancers. In contrast, *NF1* mutations rates did not differ across line of therapy, nor by *TP53* mutation status. *NF1* mutations were frequently associated with mutations in genes in the PI3K pathway (11/17 patients, 64.7%), including *PIK3CA* (6/17), *AKT1* (3/17), and *PTEN* (4/17), but rarely associated with *ESR1* mutations (1/17, 5.9%).

In the cohort, 10 of 132 primary $HR^+/HER2^-$ tumors switched phenotype to be classified as TNBC in the metastatic setting (**Fig. 2A**). These "acquired TNBC" reflected 21.7% (10/46) of advanced TNBC as a whole. The mutational profile of these "acquired TNBC" more closely resembled that of stable $HR^+/HER2^-$ tumors (both primary and recurrent $HR^+/HER2^-$) rather than stable TNBC tumors (both primary and recurrent TNBC; Supplementary Fig. 2SA), suggesting the elevated rate of *PIK3CA* mutation observed in advanced TNBC may, in part, reflect subtype switching.

Prognostic implications of genomic profiles

We investigated the influence of mutational profile on outcome, both from time of diagnosis of the original primary to relapse (disease-free survival, DFS), and the time from relapse to death (advanced overall survival, advanced OS). We note that all patients in this series relapsed, and analysis of DFS assessed risk of early versus later relapse. DFS and advanced OS data for all mutations found with a frequency of ≥5% are presented in Supplementary Tables S5 and S6, respectively. In

Table 1. The clinical demographics of the 210 patients with sequencing data from the ABC-Bio study presented by *NF1* mutation: *NF1* wild-type; *NF1*-mutant predicted truncating ($n = 9$; 6 nonsense, 2 frameshift, and 1 stop-gain); *NF1* mutant not truncating ($N = 8$; 5 missense, 2 Splice site, 1 In-frame deletion).

	NF1 wild-type $N = 193$	NF1 mutant predicted truncating $N = 9$	NF1 mutant not truncating $N = 8$	q value
Age at inclusion (years), median	56	55	51	
HR status on primary, *n* (%)				
$HR^+/HER2^-$	121 (63)	7 (78)	4 (50)	0.44[a]
$HER2^+$	23 (12)	1 (11)	1 (12)	0.98[a]
$HR^-/HER2^-$	33 (17)	1 (11)	3 (38)	0.34[a]
UK	16 (8)	0 (0)	0 (0)	NA
Total	193 (100)	9 (100)	8 (100)	
HR status on metastatic, *n* (%)				
$HR^+/HER2^-$	133 (69)	6 (67)	4 (50)	0.48[a]
$HER2^+$	16 (8)	1 (11)	2 (25)	0.27[a]
$HR^-/HER2^-$	41 (21)	2 (22)	2 (25)	0.97[a]
UK	3 (2)	0 (0)	0 (0)	
Total	193 (100)	9 (100)	8 (100)	
Presentation at diagnosis, *n* (%)				
Early	167 (87)	8 (89)	8 (100)	0.53
Metastatic	26 (13)	1 (11)	0 (0)	0.53
Total	193 (100)	9 (100)	8 (100)	
Nodal status if early presentation, *n* (%)				
Positive	100 (60)	5 (63)	6 (75)	0.72[a]
Negative	64 (38)	3 (37)	2 (25)	0.72[a]
Missing/Unknown	3 (2)	0 (0)	0 (0)	0.86
Total	167 (100)	8 (100)	8 (100)	
Germline BRCA1/2 status, *n* (%)				
Positive	12 (6)	0 (0)	1 (12)	0.49[a]
Negative	59 (31)	4 (44)	2 (25)	0.49[a]
Unknown	122 (63)	5 (56)	5 (63)	0.89
Total	193 (100)	9 (100)	8 (100)	
Adjuvant treatment if early presentation, *n* (%)				
Yes	164 (98)	8 (100)	7 (88)	0.11
No	3 (2)	0 (0)	1 (12)	0.11
Total	167 (100)	8 (100)	8 (100)	
Adjuvant ET if early presentation, *n* (%)				
Yes	123 (74)	8 (100) - 1 TNBC on primary received adjuvant ET	6 (75) - 1 TNBC on primary received adjuvant ET	0.24
No	44 (26)	0 (0)	2 (25)	0.24
Total	167 (100)	8 (100)	8 (100)	
Type of adjuvant ET if adjuvant ET, *n* (%)				
Tamoxifen only	71 (58)	6 (75)	3 (50)	0.57
AI only	19 (15)	2 (25)	1 (17)	0.77
Tamoxifen + AI	33 (27)	0 (0)	2 (33)	0.31
Total	123 (100)	8 (100)	6 (100)	
Resistance to adjuvant ET, *n* (%)				
Yes	74 (60)	6 (75)	6 (100)	0.10
No	49 (40)	2 (25)	0 (0)	0.10
Total	123 (100)	8 (100)	6 (100)	

(Continued on the following page)

Table 1. The clinical demographics of the 210 patients with sequencing data from the ABC-Bio study presented by *NF1* mutation: *NF1* wild-type; *NF1*-mutant predicted truncating ($n = 9$; 6 nonsense, 2 frameshift, and 1 stop-gain); *NF1* mutant not truncating ($N = 8$; 5 missense, 2 Splice site, 1 In-frame deletion). (Cont'd)

	NF1 wild-type $N = 193$	NF1 mutant predicted truncating $N = 9$	NF1 mutant not truncating $N = 8$	q value
Type of endocrine resistance to adjuvant ET[b], *n* (%)				
Primary resistance	23 (31)	1 (17)	1 (17)	0.59
Secondary resistance to adjuvant ET, n (%)	51 (69)	5 (83)	5 (83)	0.59
Total	74 (100)	6 (100)	6 (100)	
Prior neoadjuvant/adjuvant CT if early presentation, *n* (%)				
Yes	132 (79)	8 (100)	7 (88)	0.30
No	35 (21)	0 (0)	1 (12)	0.30
Total	167 (100)	8 (100)	8 (100)	
Prior metastatic ± adjuvant CT before sequencing, *n* (%)				
Yes	158 (82)	8 (89)	8 (100)	0.36
No	35 (18)	1 (11)	0 (0)	0.36
Total	193 (100)	9 (100)	8 (100)	
Metastatic CT after sequencing, *n* (%)				
Yes	91 (47)	3 (33)	7 (88)	0.05
No	102 (53)	6 (67)	1 (12)	0.05
Total	193 (100)	9 (100)	8 (100)	
Lines of ET therapy for metastatic disease before sequencing, *n* (%)				
0	132 (69)	9 (100)	5 (63)	0.11
1	39 (20)	0 (0)	2 (25)	0.30
2	16 (8)	0 (0)	1 (12)	NA
3+	6 (3)	0 (0)	0 (0)	NA
Total	193 (100)	9 (100)	8 (100)	
Lines of CT for metastatic disease before sequencing, *n* (%)				
0	122 (63)	8 (89)	2 (25)	**0.02**
1	36 (19)	1 (11)	3 (38)	0.34
2	21 (11)	0 (0)	1 (12)	0.57
3+	14 (7)	0 (0)	2 (25)	0.12
Total	193 (100)	9 (100)	8 (100)	

Note: Comparisons using χ^2 test.
Abbreviations: CT, chemotherapy; ET, endocrine therapy; NA, does not meet requirements for χ^2 test.
[a]Unknown excluded from analysis.
[b]Only patients with endocrine resistance considered.

patients with $HR^+/HER2^-$ tumors, truncating *NF1* mutations were associated with shorter DFS compared with wild-type *NF1* (HR 4.498, 95% CI, 1.66–12.19, log rank $P = 0.0031$; **Fig. 2B**), while *MAP3K1* mutations were associated with longer DFS (HR 0.53, 95% CI, 0.3012–0.9411, log rank $P = 0.030$). These data reflect similar poor prognosis in the adjuvant setting associated with *NF1* mutations in other datasets (12, 38). *NF1*-mutant patients had frequently received adjuvant chemotherapy (88.2%, 15/17) and adjuvant endocrine therapy (100%, 17/17). In the advanced setting, these patterns were maintained although without statistical significance (Supplementary Table S6). In patients with $HER2^+$ tumors, the 3 cancers with *HER2* mutations (both *HER2*-amplified and -mutant cancers) were associated with dramatically shorter DFS [HR 614.2, 95% CI 27.33–13803, log rank $P < 0.0001$; **Fig. 2C**). Although limited in number, these findings suggest a rare but important subset of breast cancers that may do poorly on current treatment. Interestingly, *HER2*-mutant $HR^+/HER2^-$ breast cancers also had significant worse DFS and advanced OS. Analysis of outcome for TNBC was limited by small numbers (Supplementary Tables S5 and S6).

Acquisition of NF1 mutations in ABC

We investigated whether genes mutated at higher incidence in ABC were mutated at higher incidence due to acquisition of the mutation in the metastatic setting, or whether the mutation was present in the original primary tumor but enriched in the metastatic setting due to a higher propensity to relapse. We focused our analysis on tumor samples with mutations in *NF1, AKT1*, and *HER2*–rare, but potentially targetable mutations. We did not further investigate *ESR1* mutations, as it is well documented these are acquired in the advanced setting following endocrine therapy (6, 7, 15, 30). Primary tumor samples for 34 patients were retrieved and sequenced, including samples for 13 of 17 *NF1*, 12 of

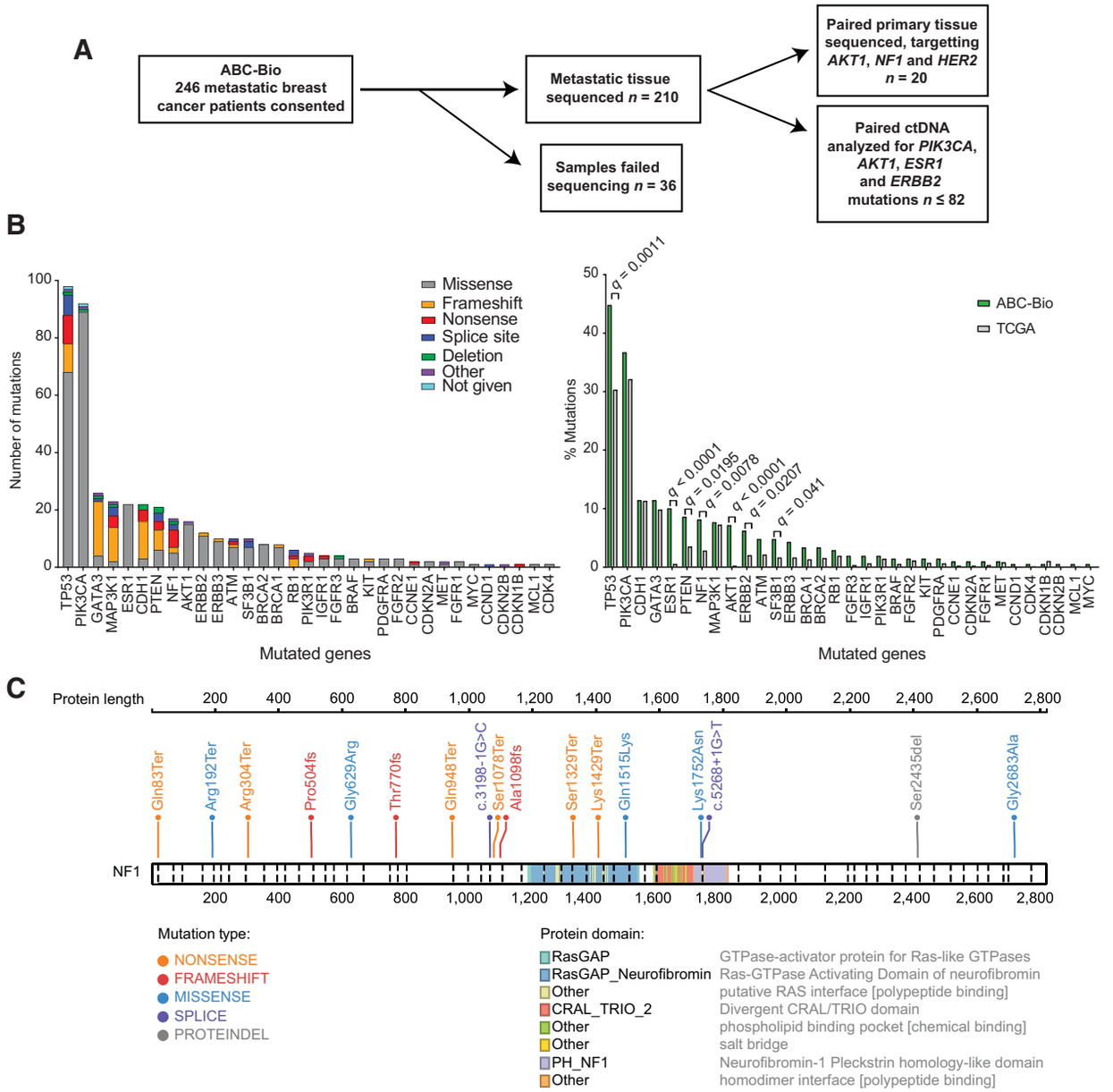

Figure 1.

Genetic profile of ABC. **A,** CONSORT diagram showing the structure and the patient numbers of the ABC-Bio clinical sequencing study. **B,** Number and type of mutations identified in ABC within ABC-Bio (left); comparison of the incidence of mutations identified in ABC-Bio (green bars) with the TCGA primary breast cancer (gray bars); *P* value was calculated by Fisher exact test with Benjamini–Hochberg false discovery correction (right). **C,** *NF1* mutations detected in the ABC-Bio study, with mutation type, functional domain, and reference to amino acid residue.

15 *AKT1*, and 6 of 12 *HER2*-mutant cases identified in the sequencing of metastatic tumors. Of the 13 patients with *NF1* mutations in their metastatic samples, 8 of 13 (61.5%) patients had *NF1* mutation in the primary tumor sample (**Fig. 2D**), indicating acquisition of *NF1* mutations continues in the advanced setting (5/13, 38.5%). In addition, one primary tissue sample was found to have an *NF1* mutation that was lost in the paired metastatic sample. In contrast, *AKT1* (10/12, 83.3%) and *HER2* (5/6, 83.3%) mutations were largely shared with the primary sample. Consistent with being truncal driver mutations, *TP53* mutations (12/13, 92.3%) were largely shared in both primary and metastatic tumor sample. *PIK3CA* mutations (5/13, 38.5%) are also acquired in the metastatic setting (26).

Gene expression analysis

Our genomic analysis suggested that *NF1* mutations may be acquired in the metastatic setting, are frequently truncating mutations predicted to inactivate *NF1* function, and are associated with marked

shorter DFS in $HR^+/HER2^-$ breast cancers with relapse during adjuvant endocrine therapy. We next investigated the functional impact of *NF1* mutations on ER-positive breast cancer.

RNA from 8 tumor samples with truncating *NF1* mutations were analyzed with a custom NanoString ER signaling gene expression codeset, along with 30 *NF1* wild-type metastatic breast cancers that had relapsed after AI therapy (ref. 15; **Fig. 3A**). Tumors with truncating *NF1* mutations had lower NF1 expression ($P = 2.74 \times 10^{-6}$, Wilcoxon signed rank test **Fig. 3B**). In the series of *NF1* wild-type cancers, 7 of 30 cancers had acquired very low ER signaling in advanced cancer (**Fig. 3A**, left branch), effectively becoming genomically ER negative. All *NF1* mutations had some maintained ER signaling (**Fig. 3A**). *ESR1* mutations have been shown to significantly increase expression of estrogen-regulated genes (ERG) and proliferation genes (15). The presence of a truncating *NF1* mutation resulted in substantially less ER signaling than *ESR1* mutations, with *NF1*-mutant cancers having broadly similar expression of ERGs and proliferation genes compared with wild-type for both *ESR1* and *NF1* ($P = 0.1572$ and $P = 0.1123$, respectively, Wilcoxon test; **Fig. 3D**). Tumors with *NF1* mutations had significantly lower expression of the nuclear corepressor proteins *NCOR1* ($P = 0.021$, Wilcoxon test) and *NCOR2* ($P = 0.011$, Wilcoxon test) than *ESR1*-mutant tumors or wild-type tumors (**Fig. 3E**). These data suggested that *NF1*-mutant tumors had downregulated ER signaling in metastases, but without the acquisition of ER-negative phenotypes prevalent in tumors wild-type for *NF1* and *ESR1* mutations.

To corroborate our findings, we analyzed gene expression and mutation data from primary tumors in TCGA. Similar to our analysis of metastatic tumors, primary tumors with truncating *NF1* mutations had decreased expression of *NF1* (Wilcoxon test, $P = 0.000159$; Supplementary Fig. S3A). Cancers with truncating *NF1* mutations had enrichment of differentially regulated genes associated with canonical estrogen receptor signaling (**Fig. 3F**), and decreased *NCOR1* compared to wild-type tumors (Supplementary Fig. S3B and S3C).

NF1 silencing results in resistance to endocrine therapy

Prior research has identified that *NF1* silencing results in resistance to tamoxifen therapy (13). Our findings on short DFS in *NF1*-mutant cancer included 14 of 17 (82.4%) patients treated with adjuvant endocrine therapy, with early relapse during endocrine therapy, suggested a potential for more general endocrine therapy resistance in the clinic. To investigate the consequence of *NF1* loss on endocrine therapy resistance, we silenced *NF1* with NF1 siRNA SMARTpool in ER-positive cell lines MCF7 and T47D, or siCON nontargeting control, and performed clonogenic assays. The individual siRNAs that comprised the SMARTpool all decreased NF1 expression (Supplementary Fig. S4A). Silencing *NF1* resulted in resistance to tamoxifen and withdrawal of estrogen from medium to mimic aromatase inhibition, with partial resistance to fulvestrant (**Fig. 4A** and **B**). Assessment using the Bliss independence model indicated that NF1 knockdown was antagonistic of endocrine therapies (Supplementary Fig. S4B)

We generated MCF7 cells with stable knockdown of *NF1* using two different shRNA constructs (shNF1-14B and shNF1-17B) and a nontargeting control (LucB; refs. 31, 32). Stable silencing of *NF1* similarly resulted in stable, long-term resistance to estrogen deprivation, fulvestrant and tamoxifen (**Fig. 4C**), despite NF1 shRNA–stable cell lines having only partial *NF1* silencing (Supplementary Fig. S4C and S4D).

We next investigated the signaling consequences of *NF1* loss and the impact on ER signaling. Silencing *NF1* using siRNA in MCF7 decreased expression of NF1 and increased levels of phospho-ERK1,2 and phospho-AKT, which was sustained when cells were treated with fulvestrant, tamoxifen, or estradiol-depleted media for 24 hours (**Fig. 4D**). However, AKT phosphorylation was also induced by NF1 loss, likely reflecting the well described role of RAS signaling in controlling PI3K activity, and suggesting that NF1 loss may possibly broadly activate both MAPK and AKT signal transduction. We performed a time-course experiment treating MCF7 cells with the MEK inhibitor, trametinib. Trametinib treatment resulted in sustained inhibited phosphorylation of ERK1,2 up to 72 hours, with strong induction of NCOR2 (Supplementary Fig. S4E). Knockdown of NF1 decreased NCOR1 and NCOR2 expression, which was increased by treatment with trametinib (Supplementary Fig. S4F). ER signaling after *NF1* silencing was investigated with RT2 profiler array (methods). *NF1* silencing downregulated *ESR1* expression (**Fig. 4E**) and ER signaling (Supplementary Fig. S4E), while upregulating CCND1 and MYC gene expression (**Fig. 4E**; Supplementary Fig. S4F). Inhibition of MEK with trametinib largely reversed the gene expression changes of *NF1* silencing (**Fig. 4E**; Supplementary Fig. S4G), implicating increased MEK–ERK signaling as the major driver of endocrine resistance.

We further investigated signaling effects of NF1 loss. *NF1* silencing resulted in increased cyclin D1 expression, which was not suppressed after 72 hours of treatment in both MCF7 and T47D cells with fulvestrant, tamoxifen, or estradiol depletion (**Fig. 5A**). *NF1* silencing did not appreciably alter the expression of cyclin E1 or E2 (**Fig. 5B**). Similarly, stable long-term knockdown of NF1 resulted in higher cyclin D1 protein expression, which was not completely suppressed by treatment with endocrine therapies (**Fig. 5B**). In keeping with elevated cyclin D1 expression, Rb phosphorylation was increased at both S780 and 807 (**Fig. 5B**), with modestly elevated phosphorylation of CDK2 T180. Cells with stable *NF1* knockdown had decreased ER expression, but increased phospho-ER, which was exaggerated compared with control when treated with tamoxifen or estradiol depletion (**Fig. 5B**). Expression of *NCOR1* and *NCOR2* were decreased in cells with stable knockdown of *NF1* (Supplementary Fig. S4D), as predicted by our tumor analysis, which was reversed by treatment with trametinib (Supplementary Fig. S4F).

In summary, *NF1* loss resulted in increased MAPK pathway signaling, that downregulated ER expression and signaling, but with residual ER hyperphosphorylation. NF1 silencing resulted in ER-independent activation of cyclin D1 expression, with increased Rb phosphorylation, suggesting that *NF1* loss promoted endocrine resistance through both ER-dependent and -independent mechanisms.

Combating NF1 loss in breast cancer therapy

We next investigated therapeutic approaches that may overcome endocrine resistance in *NF1*-mutant cancers. We noted that *NF1* silencing resulted in marked overexpression of cyclin D1 and increased RB1 phosphorylation, and we therefore investigated whether CDK4/6 inhibition may overcome the adverse effects on endocrine therapy resistance after *NF1* silencing. In short-term BrdU incorporation assays, NF1 siRNA blocked the antiproliferative effects of tamoxifen; BrdU-positive cells were reduced in control siCON cells with tamoxifen, whereas there was no reduction in siNF1 cells. Palbociclib, and the combination of palbociclib and tamoxifen, substantially reduced proliferation in siNF1 cells (**Fig. 5C**). Similarly, in long-term clonogenic assays, palbociclib reduced colony formation of MCF7 cells after *NF1* silencing and further mitigated resistance to fulvestrant, tamoxifen, and estrogen depletion (**Fig. 5D**;

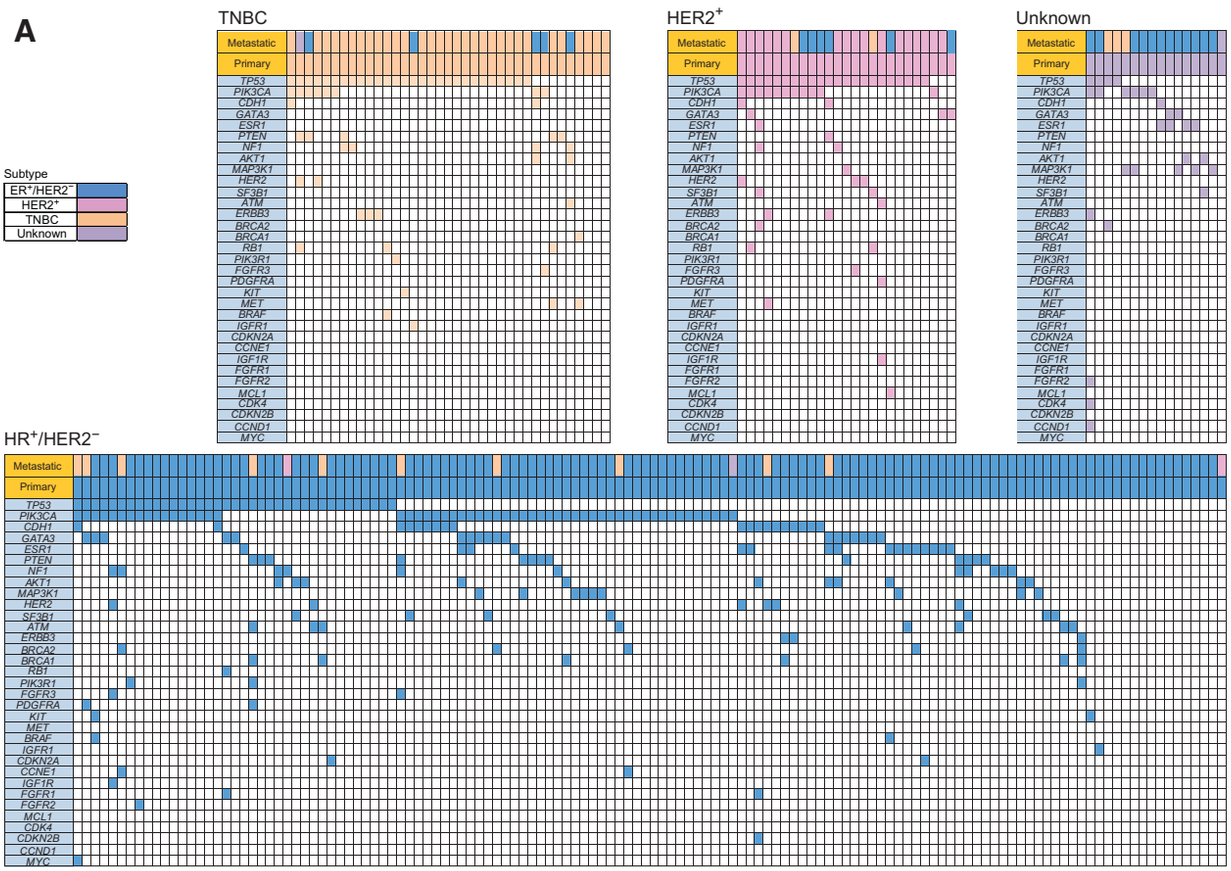

Figure 2.

Mutational profile impact on outcome and agreement with targetable mutations between paired primary and metastatic samples. **A,** Co-occurrence of mutations in metastatic setting and tumor subtype of both primary and metastatic samples, presented by subtype of primary tumor. (*Continued on the following page.*)

Supplementary Fig. S5A). Using the Bliss independence model, palbociclib was found to combine with the endocrine-targeted treatments in an additive manner (Supplementary Fig. S5B). In contrast, in cells with NF1 knockdown, the effect of combining palbociclib with the endocrine treatments was synergistic.

We then investigated the effect of *NF1* mutations on the survival in patients enrolled in the PALOMA-3 randomized phase III trial, of fulvestrant plus placebo versus fulvestrant plus palbociclib. We have previously reported ctDNA sequencing in the PALOMA-3 trial, and we analyzed the effects of *NF1* mutation detection in baseline ctDNA (39). Overall, *NF1* mutations were detected in 6.34% (21/331) baseline plasma samples. In patients with available end-of-treatment samples, the baseline *NF1* mutations (11/11) were detected at the end of treatment, suggesting stability through treatment (26, 40). Two mutations in *NF1* were selected through treatment, present at the end of treatment, but not in baseline ctDNA. There were too few patients with *NF1* mutations to make meaningful assessment in the placebo and fulvestrant control arm (Supplementary Fig. S5B). Patients with baseline *NF1* mutations detected had a similar outcome on palbociclib plus fulvestrant, compared with patients without *NF1* mutations detected (log rank, $P = 0.71$, 5/16 stopgain, 11/16 nonsynonymous; **Fig. 5E**), supporting our preclinical experiments that CDK4/6 inhibition, in part, overcame the effects of NF1 loss on endocrine resistance.

Discussion

Here we present the molecular characterization of 210 metastatic breast cancers, and demonstrate that multiple targetable mutations are detected at increased frequency in metastatic disease as compared with archival primary cancers. *NF1* mutations may be acquired in the metastatic setting and loss of *NF1* function results in resistance to all commonly used endocrine therapies, although combination of fulvestrant and CDK4/6 inhibition presents a therapeutic strategy to overcome resistance.

Our findings on acquired *NF1* mutations adds to increasing evidence that mutations in the MAPK pathway are enriched in advanced ER-positive breast cancer. We previously demonstrated that *KRAS* mutations, highly likely subclonal, may be detected at relatively high frequency after progression on AI therapy for advanced breast cancer (30). Mutations in the fibroblast growth factor receptor genes *FGFR2* and *FGFR3* may be found in ctDNA of endocrine-resistant cancers (41), with FGFR signaling canonically activating MAPK pathway signaling (42). Similarly, a large recent series of metastatic biopsy sequencing, without paired primary sequencing, demonstrated frequent mutational activation of the pathway in advanced ER-positive breast cancer (37). These data demonstrate opportunities to develop targeted therapeutic approaches. The majority of *NF1* mutations are truncating mutations, and therefore highly likely inactivating.

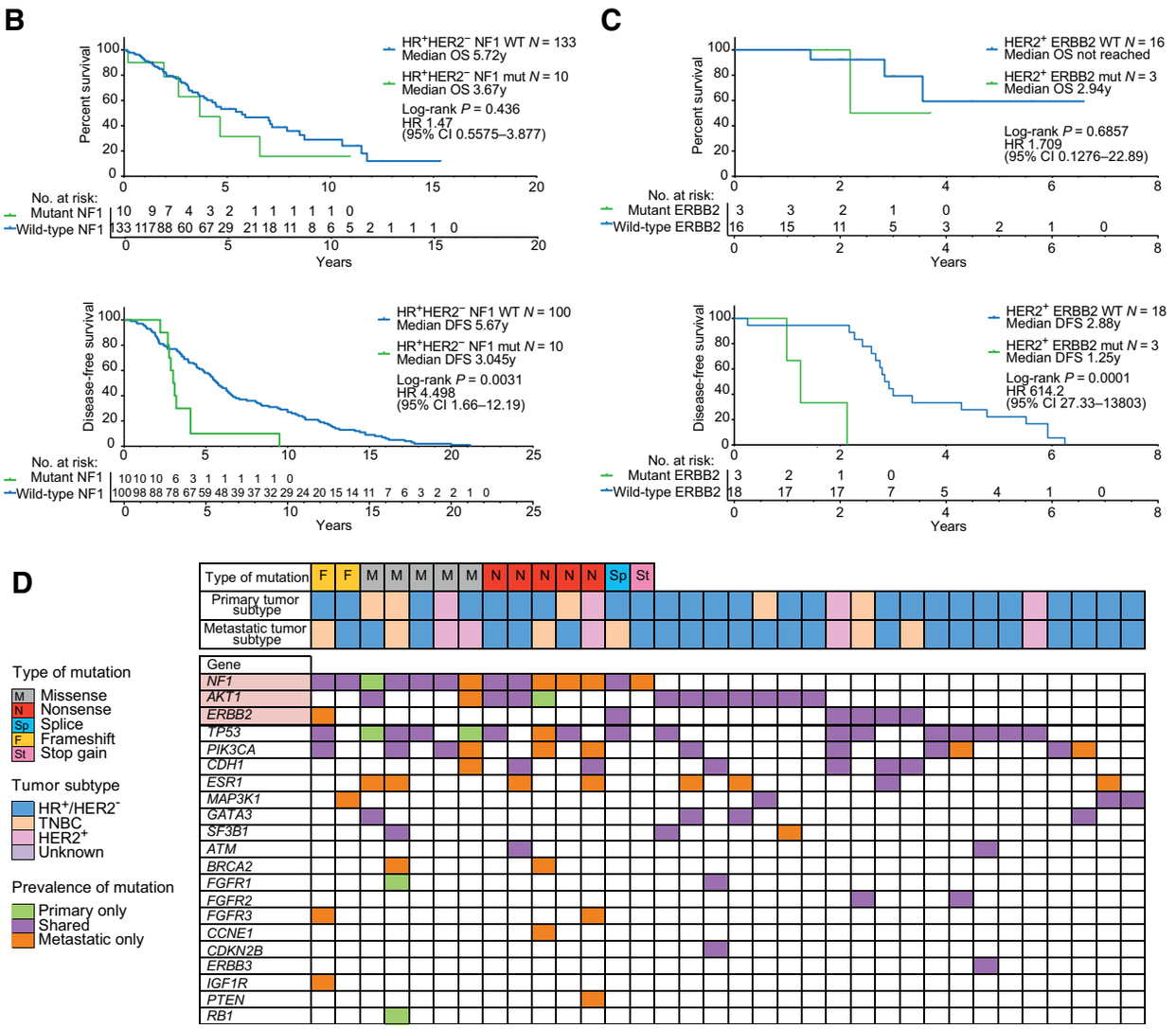

Figure 2.

(*Continued.*) **B,** *NF1* mutation status and overall survival (top) and disease-free survival – time to recurrence – (bottom) in HR^+HER2^- tumors (log-rank test, $P = 0.436$ and $P = 0.0031$ respectively). **C,** *ERBB2* mutation status and overall survival (top) and disease-free survival – time to recurrence – (bottom) in $HER2^+$ tumors (log-rank test, $P = 0.6857$ and $P = 0.0001$, respectively). **D,** Mutation concordance between primary and advanced tumor samples for 34 patients with targetable mutations in NF1, AKT1, and ERBB2 in ABC. The type of NF1 mutation and subtype of the tumor samples are indicated.

Although likely that loss of heterozygosity is required to inactivate NF1 function, our data on resistance to endocrine therapy despite only partial knockdown of NF1 with shRNA (**Fig. 4C**) suggests the possibility of heterozygous effects of NF1 loss. Missense mutations in *NF1* are relatively frequent, and although the majority of these may be nonpathogenic, further research will be required to establish whether some *NF1* missense mutations are functional. Finally, whether the clonality of these mutations is important for outcome and treatment will need to be addressed.

HR^+/HER2 breast cancer is the most frequent phenotype of breast cancer, accounting for approximately 70% of cases. *NF1* mutation confers poor prognosis in terms of shorter time to relapse in HR^+/$HER2^-$ patients, with relapse occurring frequently on endocrine therapy reflecting endocrine resistance (**Fig. 1**). Loss of NF1 results in endocrine resistance likely both through ER-dependent mechanisms and ER-independent mechanisms, likely with MAPK pathway–driven expression of cyclin D1 and ER-independent S-phase entry. Of all endocrine therapies, fulvestrant is the least resistant preclinically (**Fig. 4**). Although ER expression and signaling was partially downregulated with *NF1* silencing, residual ER was hyperphosphorylated likely reflecting ligand-independent activation of residual ER by enhanced signal transduction, which would be most effectively inhibited by fulvestrant. Combination with CDK4/6 inhibitors, which target ER independent cyclin D1 transcription (**Fig. 4**), results in substantial enhanced efficacy of endocrine therapy *in vitro* (**Fig. 5**). Consistent with these observations, the prognosis of patients with baseline or pretreatment detection of *NF1* mutation in the PALOMA-3 phase III trial (16) suggested that combined fulvestrant and palbociclib may

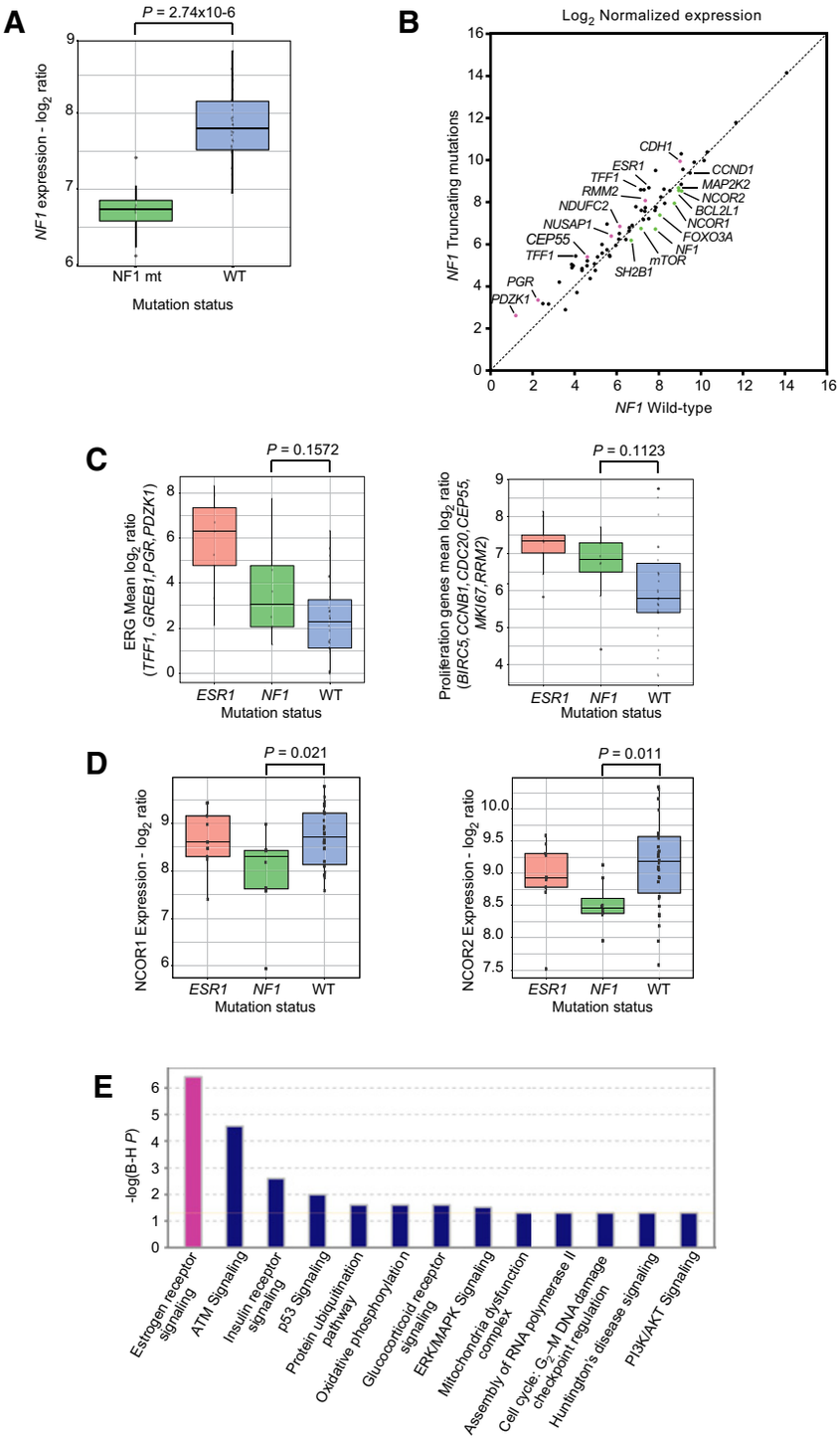

Figure 3.

Gene expression profiling of *NF1*-mutant breast cancers. **A,** Effect of truncating *NF1* mutations on *NF1* expression (log_2 ratio) compared with wild-type *NF1* tumors; *P* value as indicated, Wilcoxon test. **B,** Differential gene expression in *NF1* wild-type ($n = 30$) versus patients with truncating *NF1* mutations ($n = 8$). Indicated genes ($P < 0.1$ Wilcoxon signed rank test) with increased (•) and decreased (•) expression in truncating *NF1* mutations. **C,** Effect of *NF1* truncating mutations on averaged ER gene expression (ERG) and proliferation genes; *P* value as indicated, Wilcoxon test. **D,** Expression of the nuclear receptor corepressors in *NF1* truncating mutations, *NCOR1* (left), and *NCOR2* (right); *P* value as indicated, Wilcoxon test. **E,** Gene expression analysis of TCGA data, signaling pathways enriched for genes with differential expression in *NF1*-mutated samples (Fisher exact test, *P* value as indicated).

mitigate the adverse prognostic effects of *NF1* mutations. This suggests the possibility that fulvestrant and palbociclib could be investigated in the adjuvant setting in *NF1*-mutant cancers, in an attempt to overcome the risk of early relapse (37).

Our data has limitations; we focused our analysis of primary metastasis pairs on those potentially targetable genetic events present at increased frequency in ABC, and have therefore not performed an exhaustive investigation of discordance of genetic events. Our sequencing strategy was a targeted approach, again to investigate potential targetable genetic events, and has not interrogated genetic events outside the gene panel that would be addressed by either larger panel or whole-exome sequencing. Our analysis of the clinical impact of *NF1* mutations on fulvestrant and palbociclib is limited by small numbers, and these findings would

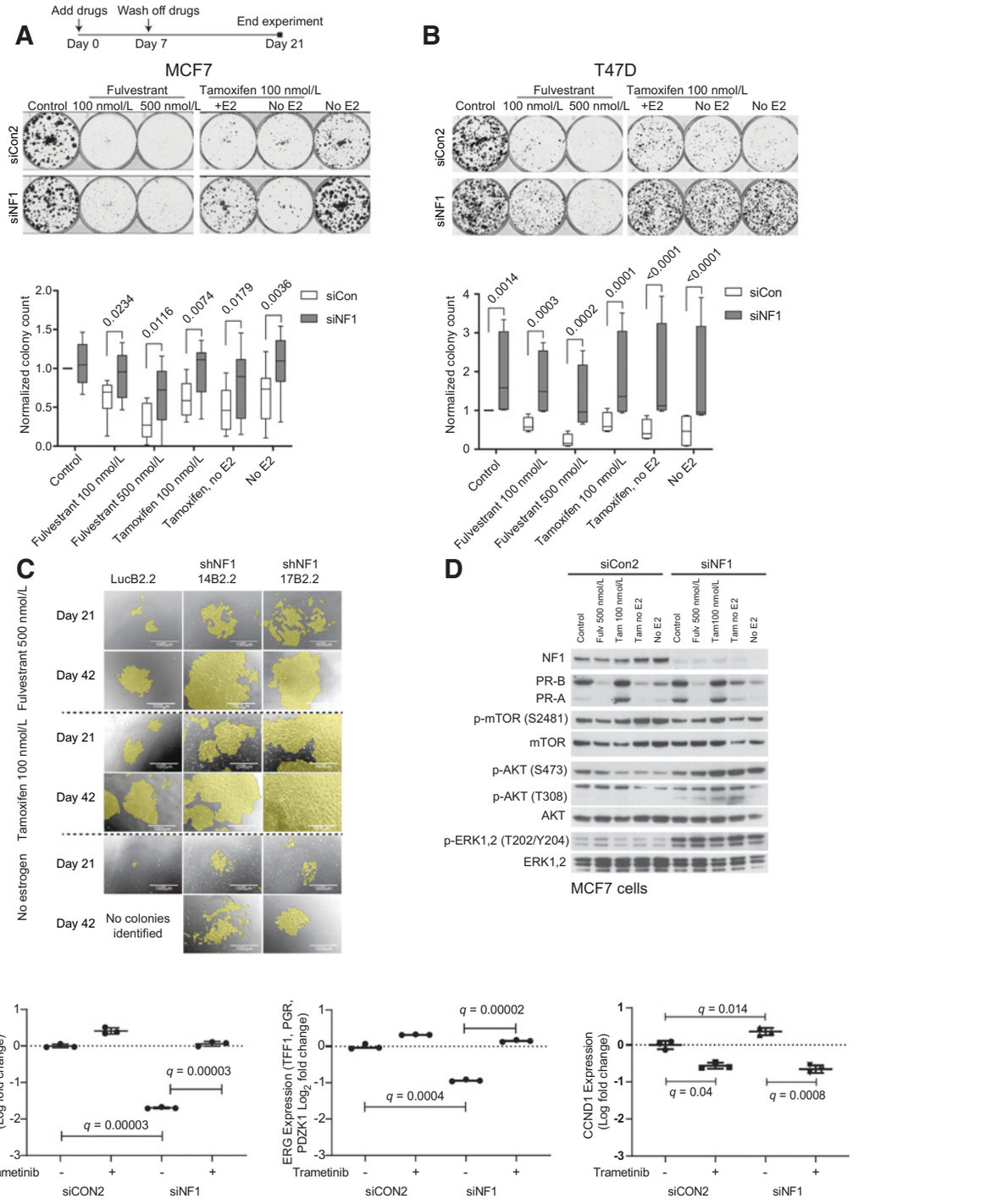

Figure 4.

Loss of NF1 causes resistance of endocrine therapy mediated by both ER-dependent and -independent mechanisms. **A,** Colony formation assay of MCF7 transfected with siCON or siNF1 and treated with either fulvestrant, tamoxifen, estradiol depletion, or control. Box, 25th–75th percentiles; bar, median; whiskers, min–max, $n = 8$; ANOVA with Sidak multiple comparisons; P values as indicated. **B,** Colony formation assay of T47D transfected with siCON or siNF1 and treated with either fulvestrant, tamoxifen, estradiol depletion, or vehicle. Box, 25th–75th percentiles; bar, median; whiskers, min–max $n = 4$; ANOVA with Sidak multiple comparisons; P values as indicated. **C,** Long-term treatment of MCF7 with stable NF1 knockdown (shNF1-14B and shNF1-17B) and control cells (LucB2.2) with fulvestrant (500 nmol/L), tamoxifen (100 nmol/L), estradiol depletion, and vehicle. Colonies highlighted in yellow. **D,** Western blot analysis of whole-cell lysates from MCF7 transfected with siCON or siNF1 and treated for 24 hours with either fulvestrant, tamoxifen, estradiol depletion, or control, and probed for the indicated proteins. **E,** Gene expression analysis of ER pathway genes in MCF7 cells transfected 96 hours earlier with indicated siRNA, treated with trametinib (100 nmol/L) or vehicle for 72 hours. q values, t test with Benjamini–Hochberg false discovery correction.

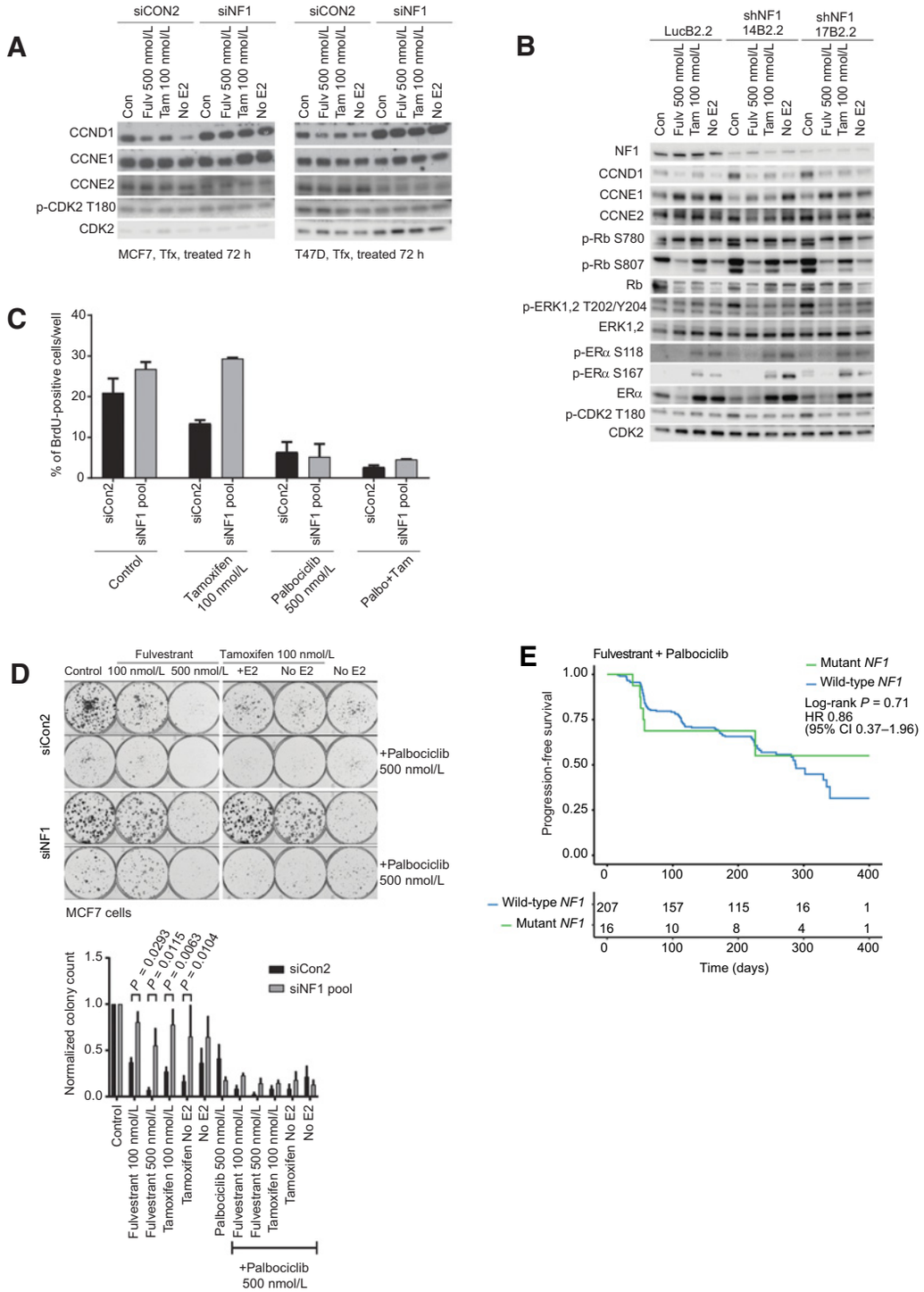

Figure 5.

CDK4/6 inhibition overcomes the adverse impact of NF1 loss in ER-positive breast cancer. **A,** Western blot of whole-cell lysates from MCF7 (left) and T47D (right), transfected with siCON or siNF1 and treated for 72 hours as indicated and probed for the indicated proteins. **B,** Western blot of whole-cell lysates from MCF7-LucB2.2, MCF7-shNF1 14B2.2, and MCF7 17B2.2, treated for 72 hours as indicated and probed for the indicated proteins. **C,** MCF7 transfected with siCON2 or siNF1, treated with tamoxifen (tam), palbociclib (palbo), combination tamoxifen + palbociclib, or vehicle for 24 hours and assessed for BrdU incorporation. **D,** Colony formation assay of MCF7 transfected with siCON or siNF1 and treated with either fulvestrant, tamoxifen, estradiol depletion, or control on their own or in combination with palbociclib. $n = 4$; two-way ANOVA with Sidak comparisons, P values as indicated. **E,** *NF1* mutation status and progression-free survival in patients enrolled in the PALOMA-3 trial treated with palbociclib and fulvestrant (log-rank test, $P = 0.71$).

need validation in additional studies of fulvestrant and CDK4/6 inhibitors. However, these studies also indicate that addition of a MEK inhibitor to CDK4/6 inhibition may offer further benefit, which could be explored in the clinic.

Breast cancers evolve through treatment, with endocrine therapy for HR-positive breast cancer driving diversification and acquisition of resistant mutations. This selection of resistance mutations presents substantial challenges to the treatment, but also opportunities to develop new therapeutic strategies. Mutations in *NF1*, both detectable in primary cancer and acquired in the metastatic setting, induce resistance to endocrine therapy, and may be targetable to reverse resistance in progressing cancers.

Disclosure of Potential Conflicts of Interest

B.A. Walker reports receiving commercial research grants from Celgene. M. Hubank is an employee/paid consultant for Guardant Health and Bristol-Myers Squibb, and reports receiving speakers bureau honoraria from Roche Diagnostics, Eli Lilly, and Coleman Research Consulting. M. Dowsett is an employee/paid consultant for Radius, Orion, and GTx, reports receiving commercial research grants from Pfizer and Radius, speakers bureau honoraria from Myriad and Roche, and other remuneration from Institute of Cancer Research. A.F.C. Okines reports receiving commercial research grants from Pfizer, and speakers bureau honoraria from Roche. S.R.D. Johnston reports receiving other commercial research support from Pfizer, Puma Biotechnology, Eli Lilly, AstraZeneca, Novartis, and Roche/Genentech, and speakers bureau honoraria from Pfizer, Novartis, Eisai, AstraZeneca, and Roche/Genentech. N.C. Turner reports receiving commercial research grants from Pfizer, and is an advisory board member/unpaid consultant for Pfizer, Novartis, and Lilly. No potential conflicts of interest were disclosed by the other authors.

Authors' Contributions

Conception and design: M. Dowsett, P. Osin, N.C. Turner

Development of methodology: P. Proszek, C. Fribbens, M.K. Shamsher, I. Garcia-Murillas, B.A. Walker, D.G. De Castro, L. Yuan

Acquisition of data (provided animals, acquired and managed patients, provided facilities, etc.): A. Pearson, P. Proszek, J. Pascual, C. Fribbens, M.K. Shamsher, B. Kingston, B. O'Leary, M.T. Herrera-Abreu, I. Garcia-Murillas, H. Bye, D.G. De Castro, L. Yuan, M. Hubank, E. Lopez-Knowles, P. Osin, A. Nerurkar, A.F.C. Okines, S.R.D. Johnston, A. Ring

Analysis and interpretation of data (e.g., statistical analysis, biostatistics, computational analysis): A. Pearson, P. Proszek, J. Pascual, M.K. Shamsher, B. O'Leary, M.T. Herrera-Abreu, R.J. Cutts, I. Garcia-Murillas, S. Jamal, M. Hubank, E.F. Schuster, M. Dowsett, P. Osin, S.R.D. Johnston, N.C. Turner

Writing, review, and/or revision of the manuscript: A. Pearson, P. Proszek, J. Pascual, C. Fribbens, B. Kingston, B. O'Leary, I. Garcia-Murillas, H. Bye, B.A. Walker, S. Jamal, E. Lopez-Knowles, E.F. Schuster, M. Dowsett, M. Parton, A.F.C. Okines, S.R.D. Johnston, A. Ring, N.C. Turner

Administrative, technical, or material support (i.e., reporting or organizing data, constructing databases): A. Pearson, P. Proszek, J. Pascual, B. Kingston, D.G. De Castro, L. Yuan

Study supervision: N.C. Turner

Acknowledgments

We would like to thank Dr. Steven Whittaker, Institute of Cancer Research, for the kind gift of the NF1 shRNA constructs, shLuc-72243, shNF1-39714, and shNF1- 39717. These studies were supported by Breast Cancer Now and NIHR funding to the Royal Marsden Hospital and Institute of Cancer Research. J. Pascual is a recipient of a grant from the Spanish Medical Oncology Society "BECA FSEOM para la formación en investigación en centros de referencia en el extranjero."

The costs of publication of this article were defrayed in part by the payment of page charges. This article must therefore be hereby marked *advertisement* in accordance with 18 U.S.C. Section 1734 solely to indicate this fact.

Received December 12, 2018; revised July 23, 2019; accepted October 2, 2019; published first October 7, 2019.

References

1. Yates LR, Knappskog S, Wedge D, Farmery JHR, Gonzalez S, Martincorena I, et al. Genomic evolution of breast cancer metastasis and relapse. Cancer Cell 2017;32:169–84.
2. Murtaza M, Dawson SJ, Pogrebniak K, Rueda OM, Provenzano E, Grant J, et al. Multifocal clonal evolution characterized using circulating tumour DNA in a case of metastatic breast cancer. Nat Commun 2015;6:8760.
3. Cancer Genome Atlas Network. Comprehensive molecular portraits of human breast tumours. Nature 2012;490:61–70.
4. Curtis C, Shah SP, Chin SF, Turashvili G, Rueda OM, Dunning MJ, et al. The genomic and transcriptomic architecture of 2,000 breast tumours reveals novel subgroups. Nature 2012;486:346–52.
5. Meric-Bernstam F, Frampton GM, Ferrer-Lozano J, Yelensky R, Perez-Fidalgo JA, Wang Y, et al. Concordance of genomic alterations between primary and recurrent breast cancer. Mol Cancer Ther 2014;13:1382–9.
6. Fribbens C, O'Leary B, Kilburn L, Hrebien S, Garcia-Murillas I, Beaney M, et al. Plasma ESR1 mutations and the treatment of estrogen receptor-positive advanced breast cancer. J Clin Oncol 2016;34:2961–8.
7. Schiavon G, Hrebien S, Garcia-Murillas I, Cutts RJ, Pearson A, Tarazona N, et al. Analysis of ESR1 mutation in circulating tumor DNA demonstrates evolution during therapy for metastatic breast cancer. Sci Transl Med 2015;7:313ra182.
8. Bollag G, Clapp DW, Shih S, Adler F, Zhang YY, Thompson P, et al. Loss of NF1 results in activation of the Ras signaling pathway and leads to aberrant growth in haematopoietic cells. Nat Genet 1996;12:144–8.
9. Madanikia SA, Bergner A, Ye X, Blakeley JON. Increased risk of breast cancer in women with NF1. Am J Med Genet A 2012;158A:3056–60.
10. Uusitalo E, Rantanen M, Kallionpaa RA, Poyhonen M, Leppavirta J, Yla-Outinen H, et al. Distinctive cancer associations in patients with neurofibromatosis type 1. J Clin Oncol 2016;34:1978–86.
11. Sharif S, Moran A, Huson SM, Iddenden R, Shenton A, Howard E, et al. Women with neurofibromatosis 1 are at a moderately increased risk of developing breast cancer and should be considered for early screening. J Med Genet 2007;44:481–4.
12. Griffith OL, Spies NC, Anurag M, Griffith M, Luo J, Tu D, et al. The prognostic effects of somatic mutations in ER-positive breast cancer. Nat Commun 2018;9:3476.
13. Mendes-Pereira AM, Sims D, Dexter T, Fenwick K, Assiotis I, Kozarewa I, et al. Genome-wide functional screen identifies a compendium of genes affecting sensitivity to tamoxifen. Proc Natl Acad Sci U S A 2012;109:2730–5.
14. Arnedos M, Drury S, Afentakis M, A'Hern R, Hills M, Salter J, et al. Biomarker changes associated with the development of resistance to aromatase inhibitors (AIs) in estrogen receptor-positive breast cancer. Ann Oncol 2014;25:605–10.
15. Lopez-Knowles E, Pearson A, Schuster G, Gellert P, Ribas R, Yeo B, et al. Molecular characterisation of aromatase inhibitor-resistant advanced breast cancer: the phenotypic effect of ESR1 mutations. Br J Cancer 2019;120:247–55.
16. Turner NC, Huang Bartlett C, Cristofanilli M. Palbociclib in hormone-receptor-positive advanced breast cancer. N Engl J Med 2015;373:1672–3.
17. Stephens PJ, Tarpey PS, Davies H, Van Loo P, Greenman C, Wedge DC, et al. The landscape of cancer genes and mutational processes in breast cancer. Nature 2012;486:400–4.
18. Lawrence MS, Stojanov P, Mermel CH, Robinson JT, Garraway LA, Golub TR, et al. Discovery and saturation analysis of cancer genes across 21 tumour types. Nature 2014;505:495–501.
19. Ramos AH, Lichtenstein L, Gupta M, Lawrence MS, Pugh TJ, Saksena G, et al. Oncotator: cancer variant annotation tool. Hum Mutat 2015;36:E2423–9.
20. Chen X, Schulz-Trieglaff O, Shaw R, Barnes B, Schlesinger F, Kallberg M, et al. Manta: rapid detection of structural variants and indels for germline and cancer sequencing applications. Bioinformatics 2016;32:1220–2.
21. Klonowska K, Czubak K, Wojciechowska M, Handschuh L, Zmienko A, Figlerowicz M, et al. Oncogenomic portals for the visualization and analysis of genome-wide cancer data. Oncotarget 2016;7:176–92.

22. Lawrence MS, Stojanov P, Polak P, Kryukov GV, Cibulskis K, Sivachenko A, et al. Mutational heterogeneity in cancer and the search for new cancer-associated genes. Nature 2013;499:214–8.
23. Robinson JT, Thorvaldsdottir H, Winckler W, Guttman M, Lander ES, Getz G, et al. Integrative genomics viewer. Nat Biotechnol 2011;29:24–6.
24. Thorvaldsdottir H, Robinson JT, Mesirov JP. Integrative Genomics Viewer (IGV): high-performance genomics data visualization and exploration. Brief Bioinform 2013;14:178–92.
25. McKenna A, Hanna M, Banks E, Sivachenko A, Cibulskis K, Kernytsky A, et al. The Genome Analysis Toolkit: a MapReduce framework for analyzing next-generation DNA sequencing data. Genome Res 2010;20:1297–303.
26. O'Leary B, Hrebien S, Morden JP, Beaney M, Fribbens C, Huang X, et al. Early circulating tumor DNA dynamics and clonal selection with palbociclib and fulvestrant for breast cancer. Nat Commun 2018;9:896.
27. Hrebien S, O'Leary B, Beaney M, Schiavon G, Fribbens C, Bhambra A, et al. Reproducibility of digital PCR assays for circulating tumor DNA analysis in advanced breast cancer. PLoS One 2016;11:e0165023.
28. Pender A, Garcia-Murillas I, Rana S, Cutts RJ, Kelly G, Fenwick K, et al. Efficient genotyping of KRAS mutant non-small cell lung cancer using a multiplexed droplet digital PCR approach. PLoS One 2015;10:e0139074.
29. Pearson A, Smyth E, Babina IS, Herrera-Abreu MT, Tarazona N, Peckitt C, et al. High-level clonal FGFR amplification and response to FGFR inhibition in a translational clinical trial. Cancer Discov 2016;6:838–51.
30. Fribbens C, Garcia Murillas I, Beaney M, Hrebien S, O'Leary B, Kilburn L, et al. Tracking evolution of aromatase inhibitor resistance with circulating tumour DNA analysis in metastatic breast cancer. Ann Oncol 2018;29:145–53.
31. Whittaker SR, Cowley GS, Wagner S, Luo F, Root DE, Garraway LA. Combined Pan-RAF and MEK inhibition overcomes multiple resistance mechanisms to selective RAF inhibitors. Mol Cancer Ther 2015;14:2700–11.
32. Whittaker SR, Theurillat JP, Van Allen E, Wagle N, Hsiao J, Cowley GS, et al. A genome-scale RNA interference screen implicates NF1 loss in resistance to RAF inhibition. Cancer Discov 2013;3:350–62.
33. Asghar US, Barr AR, Cutts R, Beaney M, Babina I, Sampath D, et al. Single-cell dynamics determines response to CDK4/6 inhibition in triple-negative breast cancer. Clin Cancer Res 2017;23:5561–72.
34. Herrera-Abreu MT, Palafox M, Asghar U, Rivas MA, Cutts RJ, Garcia-Murillas I, et al. Early adaptation and acquired resistance to CDK4/6 inhibition in estrogen receptor-positive breast cancer. Cancer Res 2016; 76:2301–13.
35. Cerami E, Gao J, Dogrusoz U, Gross BE, Sumer SO, Aksoy BA, et al. The cBio cancer genomics portal: an open platform for exploring multidimensional cancer genomics data. Cancer Discov 2012;2:401–4.
36. Gao J, Aksoy BA, Dogrusoz U, Dresdner G, Gross B, Sumer SO, et al. Integrative analysis of complex cancer genomics and clinical profiles using the cBioPortal. Sci Signal 2013;6:pl1.
37. Razavi P, Chang MT, Xu G, Bandlamudi C, Ross DS, Vasan N, et al. The genomic landscape of endocrine-resistant advanced breast cancers. Cancer Cell 2018;34: 427–38.
38. Pereira B, Chin S-F, Rueda OM, Vollan H-KM, Provenzano E, Bardwell HA, et al. The somatic mutation profiles of 2,433 breast cancers refine their genomic and transcriptomic landscapes. Nat Commun 2016;7:11479.
39. O'Leary B, Finn RS, Turner NC. Treating cancer with selective CDK4/6 inhibitors. Nat Rev Clin Oncol 2016;13:417–30.
40. O'Leary B, Cutts RJ, Liu Y, Hrebien S, Huang X, Fenwick K, et al. The genetic landscape and clonal evolution of breast cancer resistance to palbociclib plus fulvestrant in the PALOMA-3 trial. Cancer Discov 2018;8:1390–403.
41. Garcia-Murillas I, Proszek P, Fribbens C, L Yuan L, Bye H, M Hubank M, et al. Circulating tumor DNA analysis with ultra-high sensitivity sequencing in metastatic breast cancer [abstract]. In: Proceedings of the 2017 San Antonio Breast Cancer Symposium; 2017 Dec 5–9; San Antonio, TX. Philadelphia (PA): AACR; 2018. Abstract nr P2-02-17.
42. Babina IS, Turner NC. Advances and challenges in targeting FGFR signalling in cancer. Nat Rev Cancer 2017;17:318–32.